

Experimental analysis of decoherence in a CV bi-partite systems

D. Buono,^{1,*} G. Nocerino,^{1,†} A. Porzio,^{2,3,‡} and S. Solimeno^{3,§}

¹*Facoltà di Scienze MM. FF. NN., Università di Salerno, via Ponte don Melillo - 84084 - Fisciano (SA)*

²*CNR - SPIN, Napoli*

³*Dipartimento di Scienze Fisiche, Università "Federico II",
Complesso Univ. Monte Sant'Angelo, I-80126 Napoli, Italy.*

Quantum properties are soon subject to decoherence once the quantum system interacts with the classical environment. In this paper we experimentally test how propagation losses, in a Gaussian channel, affect the bi-partite Gaussian entangled state generated by a sub-threshold type-II optical parametric oscillator (OPO). Experimental results are discussed in terms of different quantum markers, as teleportation fidelity, quantum discord and mutual information, and continuous variable (CV) entanglement criteria. To analyse state properties we have retrieved the composite system covariance matrix by a single homodyne detector. We experimentally found that, even in presence of a strong decoherence, the generated state never disentangles and keeps breaking the quantum limit for the discord. This result proves that the class of CV entangled states discussed in this paper would allow, in principle, to realize quantum teleportation over an infinitely long Gaussian channel.

PACS numbers: 03.65Ud, 03.67.Mn, 42.50.Ex

I. INTRODUCTION

“Quantumness” is very fragile and its surviving over long distances and times is subtly interconnected to the amount of noise coupling into the quantum system through its unavoidable interaction with the classical environment. Among the different quantum signatures, entanglement, a concept firstly introduced by Schrödinger [1] in response to the famous Einstein, Podolsky and Rosen paper in 1935 [2], probably represents the most fascinating one. The conceptual consequences of entanglement are somehow subtle and deeply affect many aspects of modern physics as the interaction between reality and observer [3], the actual limit for defining metrology standards [4], the limit to communication security [5].

The optical realization of such an intriguing quantum feature has gained, in the last decades, a central role for realising complex quantum communication protocols [6]. Among the different approaches the use of bright beams, *i.e.* optical modes carrying many photons, appears as the most robust carrier of entangled information [7] no matter if the latter will be coded into single-photon-like states (discrete quantum coding) or over the quadratures of the carrier beams (continuous valued quantum coding) [8].

By interacting with the external world, a pure quantum state decoheres into a mixture [9] and its quantumness, if not completely death [10], need to be restored or re-enhanced by suitable protocols [11]. As a matter of fact, decoherence limits both the attainable protocol fidelity and the type of accessible protocols.

The aim of this paper is to discuss and experimentally analyse the effects of the transmission over a lossy channel on the quantumness of bi-partite Gaussian continuous variable (CV) optical entangled states. While these effects on CV entangled states obtained by above threshold OPOs have been already investigated [12], we focus our analysis on the states generated by a type-II sub-threshold OPO [13].

The birth of an entangled state happens whenever a genuine quantum correlation, *i.e.* without classical analogue, is set between two distinguishable quantum systems. This implies that the system wavefunction cannot factorize into the product of wavefunctions of the single sub-systems. While this definition is almost unique entanglement marks itself into different properties of the quantum state of the whole system and can be seen under different perspectives [14]. For this reason, since the first experimental demonstration of entanglement [15] several criteria and quantities have been introduced for analyzing *entanglementness* [16, 17]. Furthermore, the definition of an entangled state is conceptually connected to pure states [18]. The properties of these states are described by wave functions and *gedanken* experiments can be though for testing different theoretical aspects but we all know that the states we can prepare

*Electronic address: danielabuono@yahoo.com

†Electronic address: gaetanocerino@libero.it

‡Electronic address: alberto.porzio@spin.cnr.it

§Electronic address: solimeno@na.infn.it

and manipulate in the laboratory are not pure but mixed. So that, experimental entanglement tests, especially in CV regime, are described in terms of density matrices rather than wavefunctions. Far from the ideal concept of pure states and systems that do not interact with the environment and/or observers, any quantum state undergoes to decoherence phenomena. In optics the most common process leading to decoherence is the phase insensitive loss of photons through diffusion and absorption mechanisms. This process is described by a Lindblad equation [19] for the evolution of the field operators that translates into a Master equation for the state density matrix. Eventually, if the state is Gaussian, *i.e.* its Wigner function is Gaussian, it admits a full description in term of its covariance matrix [20].

The investigated CV entangled state represents one of the possible quantum resources in CV teleportation protocols [21]. The experimental data we present extend the analysis of Ref. [22] discussing the behaviour of the CV entangled system to the strong decoherence regime (up 99% of loss). Moreover, we discuss in details the relationship between the three different entanglement criteria used in the CV field linking them to the teleportation fidelity and quantum discord, two possible quantum signatures for evaluating the possibility of using this class of states in quantum communication protocols [23, 24]. The discussion on the experimental results is preceded by a detailed theoretical foreword aimed at giving a physical insight the different criteria and quantities actually used for classifying CV entanglement. With this paper we prove that the state we are able to generate never disentangles. This rather counter-intuitive result has also been shown theoretically for the case of qubits states, showing a purity at the generation stage above a threshold value [25]. Moreover, the state we analyse can be used as the quantum resource for an effective quantum teleportation, of a coherent state, for any value of the transmission loss although the teleportation fidelity slowly reduce to its quantum limit.

Optical entangled states can be obtained in non-linear processes such as parametric amplifiers that, depending on their operating regime, can prepare either single photon [26] or continuous variable Gaussian entangled states [27–30]. In the latter case the non-linear medium is allocated in a optical cavity and the OPOs, below the oscillation threshold and in a semiclassical approach, are described by bilinear Hamiltonians so realising the paradigm for Gaussian state generation [31]. In particular below threshold a single continuous wave OPO, generating squeezing in a fully degenerate operation [32], can give raise to a pair of bright CV entangled beams in the non-degenerate case [29, 30, 33–35]. Both the cases lead to states that represent robust resources for implementing different quantum communication tasks [36].

In this paper we experimental discuss the behaviour, under strong loss, of a bright bi-partite CV Gaussian entangled state outing a sub-threshold type-II OPO. In particular, we analyse, for this state, the behaviour of different quantumness and entanglement markers in order to discuss the limit at which this state can be transmitted before loosing its quantum ability of being employed in quantum communication protocols. More in details, we discuss: state purity, mutual information, quantum discord and three different entanglement criteria: Peres–Horodechi–Simon [37, 38], Duan [39], and EPR–Reid [16]. In addition we relate these criteria to the teleportation fidelity \mathcal{F} , *i.e.* the state ability of overcoming the quantum limit in a teleportation protocol for a coherent state.

These states, already successfully generated in the laboratories [13, 27, 29], are Gaussian, *i.e.* they are completely characterized by their covariance matrix, namely, by the first and second moments of their quadratures so that they can be easily characterized by a single homodyne detector [40].

The paper is organized as follows: first, in Sect. II a general overview over the state generated by a sub-threshold OPO is given and the model for its evolution in a lossy Gaussian channel is discussed. In Sect. III the different entanglement markers are introduced in terms of the state covariance matrix. The section includes a detailed discussion on the relationship between the different entanglement criteria and quantum markers for CV Gaussian states. Next, in Sect. IV the quantum markers' evolution in term of channel transmission is given. A brief description of the experimental apparatus, given in Sect. V, precedes the discussion, in Sect. VI, of our experimental findings. Eventually, in Sect. VII, conclusions are drawn.

II. GAUSSIAN CV BI-PARTITE SYSTEM

A sub-threshold frequency degenerate type-II OPO generates a bi-partite state made of the two downconverted cross-polarized beams [41]. These states are Gaussian *i.e.* the Wigner function (W) of the state ρ , expressed in terms of field quadratures is Gaussian. In our case, we can assume that the average values of quadratures to be zero [13] so that we can write W as

$$W(\mathbf{K}) = \frac{\exp\left[-\frac{1}{2}\mathbf{K}^T\sigma^{-1}\mathbf{K}\right]}{\pi^2\sqrt{\text{Det}[\sigma]}}, \quad (1)$$

where $\mathbf{K} \equiv (X_1, Y_1, X_2, Y_2)^T$ is the vector of the field quadratures (hereafter, whenever not necessary, we will omit the " $\hat{}$ " on operators so that: $X = (a^\dagger + a)/\sqrt{2}$ and $Y = i(a^\dagger - a)/\sqrt{2}$) for mode 1 and 2 respectively.

A Gaussian state can be fully characterized by the matrix of the second order statistical moments of the field quadratures, *i.e.* the covariance matrix (**CM**) σ , whose elements are defined by $\sigma_{kh} \equiv \frac{1}{2} \langle \{K_k, K_h\} \rangle - \langle K_k \rangle \langle K_h \rangle$ where $\{K_k, K_h\} = K_k K_h + K_h K_k$. Moreover, for a bi-partite field state, σ can be always given in the standard form by local symplectic operations

$$\sigma = \begin{pmatrix} \alpha & \gamma \\ \gamma^\top & \beta \end{pmatrix} = \begin{pmatrix} n & 0 & c_1 & 0 \\ 0 & n & 0 & c_2 \\ c_1 & 0 & m & 0 \\ 0 & c_2 & 0 & m \end{pmatrix}, \quad (2)$$

where α , β and γ are 2×2 real matrices, representing respectively the self and mutual correlations matrices. The quantities, n , m , c_1 and c_2 are determined by the four local symplectic invariants $I_1 \equiv \det(\alpha) = n^2$, $I_2 \equiv \det(\beta) = m^2$, $I_3 \equiv \det(\gamma) = c_1 c_2$, $I_4 \equiv \det(\sigma) = (nm - c_1^2)(nm - c_2^2)$. We note that the experimental matrices we have measured and that will be discussed in Sect. VI are all in the above standard form. As a matter of fact, a sub-threshold type-II OPO, due to the symmetry of its Hamiltonian, can only produce states of this kind. So that, hereafter, whenever we refer to **CM** we will intend a covariance matrix in the standard form of Eq. (2). Moreover, at the time of their birth, states produced in an OPO show $n = m$ and $c_1 = -c_2$, and the matrix is called symmetric and represents a bi-partite state where the energy is equally distributed between the two modes.

σ is a *bona fide* **CM** *i.e.* it describes a physical state iff

$$\sigma + \frac{i}{2} \omega \oplus \omega \geq 0, \quad (3)$$

where $\omega \equiv \begin{pmatrix} 0 & 1 \\ -1 & 0 \end{pmatrix}$. The above condition can be written in terms of the four symplectic invariants

$$I_1 + I_2 + 2I_3 \leq 4I_4 + \frac{1}{4}. \quad (4)$$

The above inequalities are equivalent to the Heisenberg uncertainty principle for a two-mode state and to ask covariance matrix positivity.

The **CM** is also characterized by its symplectic eigenvalues

$$d_{\pm} = \sqrt{\frac{I_1 + I_2 + 2I_3 \pm \sqrt{(I_1 + I_2 + 2I_3)^2 - 4I_4}}{2}}. \quad (5)$$

Inequality (4) assumes a simple form in term of d_- :

$$d_- \geq \frac{1}{2}.$$

We also note that a Gaussian pure state is a minimum uncertainty state and that the **CM** relative to a pure state necessary has $\det(\sigma) = I_4 = 1/16$ (see Eq. (11) below) so that the case $c_1 = -c_2 = c$ implies $n = m$, to ensure a *bona fide* **CM**, and for a pure fully symmetric state

$$c = \sqrt{n^2 - 1/4}. \quad (6)$$

Moreover, for mixed fully symmetric states, $c \leq \sqrt{n^2 - 1/4}$ with the inequality saturated only by pure states. Hereafter we will indicate these fully symmetric states as *diagonal*. The meaning of this name will be clarified in Sect. III.

A. Evolution in a lossy Gaussian channel

Decoherence indicates the detrimental effect on a quantum system that stochastically interacts with the external world. The state of the system, initially pure, becomes mixed. In the density matrix language it translates into the fact that while a pure state is represented by an idempotent density matrix ρ ($\rho^2 = \rho$) this is not true for a decohered mixed state. The lossy transmission of an arbitrary optical quantum state between two sites is an irreversible decoherence process that can be described by using the open systems approach [19]. In this approach the environment is seen as a reservoir (thermal bath) made up of infinite modes at thermal equilibrium. The Kossakowski-Lindblad equation describes the time evolution in a noisy quantum channel of a multi-mode quantum state ρ_S . This model is valid if the system S and the reservoir R satisfy the following general conditions:

- *weak coupling (Born approximation)* – the coupling between system and environment is so that the density matrix ρ_R of the environment is negligibly influenced by the interaction (the thermal bath state is stationary). This approximation allows to write the state $\rho_{SR}(t)$ of the global system as $\rho_{SR}(t) \approx \rho_S(t) \otimes \rho_R$;
- *Markovianity* – there are not memory effects neither on the system and the reservoir. This approximation implies that the time scale τ over which $\rho_S(t)$ changes appreciably under the influence of the bath is large compared to the time scale τ_R over which the bath forgets about its past, $\tau \gg \tau_R$.
- *Secularity (rotating wave approximation)* – the typical time scale τ_S of the intrinsic evolution of the system S is small compared to the relaxation time τ . For an optical field it implies that the reservoir reacts to the average field and not to its instantaneous value.

The evolution of an arbitrary two-mode Gaussian state in a noisy channel, at thermal equilibrium, can be translated into the formalism of the Wigner function obtaining the following Fokker-Planck equation for $W(\mathbf{K})$ (see Eq.(1)) [9],

$$\partial_t W(\mathbf{K}, t) = \frac{\Gamma}{2} \left(\partial_{\mathbf{K}}^{\top} \mathbf{K} + \frac{1}{2} \nabla_{\mathbf{K}}^2 \right) W(\mathbf{K}) , \quad (7)$$

where Γ is the damping rate of the channel for both modes, while $\partial_{\mathbf{K}}^{\top} = (\partial_{X_1}, \partial_{Y_1}, \partial_{X_2}, \partial_{Y_2})$ and $\nabla_{\mathbf{K}}^2 = \partial_{\mathbf{K}}^{\top} \partial_{\mathbf{K}} = \partial_{X_1}^2 + \partial_{Y_1}^2 + \partial_{X_2}^2 + \partial_{Y_2}^2$.

The evolution of Eq.(7) preserves the Gaussian character of the initial state and in terms of the **CM** σ reads

$$\sigma(t) = (1 - e^{-\Gamma t}) \frac{1}{2} \mathbb{I} + e^{-\Gamma t} \sigma(0), \quad (8)$$

where $\sigma(0)$ is the covariance matrix at $t = 0$ and \mathbb{I} is the 4×4 identity matrix ($\frac{1}{2}\mathbb{I}$ is the vacuum state covariance matrix setting the standard quantum limit SQL).

This form is in all equal to the effects of a fictitious beam-splitter (BS) that mimics the channel losses and couples into the system the vacuum quantum noise through its unfilled port. Being $U_k(\zeta) = \exp\left\{\zeta \left(a_k^\dagger v_k - v_k^\dagger a_k\right)\right\}$ the SU(2) transformation induced by the BS on the k -mode ($k = 1, 2$, with v_k the modal operator for the vacuum) and $T = e^{-\Gamma t}$ the power transmission of the beam splitter ($\tan \zeta = \sqrt{(1-T)/T}$), the above equation becomes:

$$\sigma_T = (1 - T) \frac{1}{2} \mathbb{I} + T \sigma_1 . \quad (9)$$

In this form we can drop the temporal dependence and label the **CM** of the initial state as $\sigma_{T=1} \equiv \sigma_1$. For states in the form of Eq. (2) the different elements evolve as

$$\begin{aligned} n_T &= \frac{1}{2} + T \left(n - \frac{1}{2} \right) \\ m_T &= \frac{1}{2} + T \left(m - \frac{1}{2} \right) \\ c_{1(2),T} &= c_{1(2)} T \end{aligned} \quad (10)$$

For an infinite transmission channel $T \rightarrow 0$ implies $\sigma_T \rightarrow \frac{1}{2}\mathbb{I}$ *i.e.* the fully decohered **CM** represents a two-mode vacuum state.

III. QUANTUM MARKERS AND ENTANGLEMENT

The quantumness of a bi-partite **CV** state can be tested by two classes of markers. The first is intimately related to the state itself and includes inequalities that fix bounds for distinguishing among entangled and un-entangled states. The second has been translated into the quantum context from the classical information theory and is related to the amount of quantum information carried by the state. The latter includes quantitative measures such as mutual information, von Neumann entropy, quantum discord and teleportation fidelity. The former is made of entanglement criteria usually named by the authors that have theoretically found them. They are the PHS (Peres-Horodecki-Simon) [37, 38], Duan[39], EPR-Reid [16] criteria. Before going into details it is useful to start by introducing the state purity as an extra marker that tells how far the analysed state is from a pure one.

1. State purity

Every quantum information protocol and every measurement scheme must take into account the fact that pure states are inevitably corrupted by the interaction with the environment and, therefore, in real experiments only mixed states are available. The purity $\mu = \text{Tr}[\rho^2]$ ($\mu < 1$ for mixed state, $= 1$ for pure) may be expressed as a function of the **CM** (2) being

$$\mu = \frac{1}{4\sqrt{\det[\sigma]}}. \quad (11)$$

Intimately related to the purity, it is possible to introduce the von Neumann entropy $S(\rho)$. It is zero for pure states while strictly positive for mixed ones. In the case of the two-mode Gaussian state the entropy $S(\rho)$ can be written in terms of its covariance matrix symplectic eigenvalues d_{\pm} (see Eq. (5)) as $S(\rho) = f(d_+) + f(d_-)$ [42] where

$$f(x) = (x + 1/2) \log(x + 1/2) - (x - 1/2) \log(x - 1/2). \quad (12)$$

We note that both μ and $S(\rho)$ are invariant under symplectic transformations.

A. Entanglement criteria

Although it has not been found a general solution to the problem of a quantitative measure of entanglement for mixed states, there exist necessary and sufficient conditions to assess whether a given state is entangled or not. These criteria provide a test for entanglement, and can be employed for studying the behaviour of entanglement in a quantum transmission channel.

1. The Peres-Horodecki-Simon (PHS) criterion

A bi-partite quantum state is separable iff its density operator can be written as a convex combination of the tensor product of density operators relative to the two different sub-systems [43]

$$\rho = \sum_j p_j \rho_{j1} \otimes \rho_{j2}, \quad (13)$$

where $\sum_j p_j = 1$ while ρ_{ji} $i = 1, 2$ are the density matrices of subsystems 1 and 2. By performing a partial transposition (*i.e.* transposition of the density matrix with respect to only one of the two Hilbert subspaces) ρ transforms into ρ_{PT} . In the case ρ is a separable state, ρ_{PT} should still represent a physical state so that ρ_{PT} must be a non-negative density operator. On the contrary if ρ_{PT} no more represents a physical state the system does not admit the form (13). Thus, all separable states have a non-negative partially transposed density operator. From this consideration it is possible to deduce a necessary condition for separability or viceversa a sufficient condition for entanglement. In view of this the criterion is sometime referred to as the *ppt* criterion (*positivity* under *partial transposition*) [37, 38]. In the following we prefer to indicate it as the PHS criterion. It can be proven that it becomes a necessary and sufficient condition for Gaussian states [38]. From the **CM** point of view, partial transposition implies a sign flip for I_3 so that PHS criterion has a simple expression in terms of **CM** elements: a bi-partite Gaussian state is separable iff

$$n^2 + m^2 + 2|c_1 c_2| - 4(nm - c_1^2)(nm - c_2^2) \leq \frac{1}{4}, \quad (14)$$

and it is entangled otherwise. We also note that the PHS criterion is invariant under symplectic transformations.

PHS criterion relies on the possibility of describing independently the two subsystems. In phase space, transposition is defined as “time reversal” (or mirror reflection), which is given by a change of sign of out-of-phase quadrature (usually indicated as Y). Partial transposition is, therefore, a “local time reversal” which inverts the Y quadrature of only one subsystem. If any *true quantum* correlation is set between Y_1 and Y_2 a sign flip on Y_1 (or Y_2) will affect the sign of c_1 (or c_2) in Eq. (2) making ρ_{PT} no more physical (see Eq. (4)).

2. The Duan criterion

For every bi-partite state there exists a pair of EPR-like conjugate operators defined by

$$\hat{u} = |a| \hat{x}_1 + \frac{1}{a} \hat{x}_2 \text{ and } \hat{v} = |a| \hat{p}_1 - \frac{1}{a} \hat{p}_2, \quad (15)$$

with a an arbitrary non-zero real number and $[\hat{x}_j, \hat{p}_{j'}] = \frac{i}{2} \delta_{jj'}$ ($j, j' = 1, 2$) and where subscript refers to the 1 (2) subsystem. Then, the birth of non-classical correlation between sub-systems 1 and 2 will lead to states for which the variance of EPR-like operators will reduce below the standard quantum limit (SQL). By calculating the total variance of such a pair of operators on ρ , a separable state of the form of Eq. (13), it can be proven [39] that

$$\langle (\Delta \hat{u})^2 \rangle_\rho + \langle (\Delta \hat{v})^2 \rangle_\rho \geq a^2 + \frac{1}{a^2}, \quad (16)$$

setting a lower bound for separable states. Contrarily to the PHS criterion (see Sect. III A 1) inequality (16) has been formulated only as a necessary condition for separability so that it is a sufficient condition for entanglement of a generic CV Gaussian state.

As shown in [39] it becomes a necessary and sufficient condition for entangled CV Gaussian states. The sufficient and necessary condition can be expressed in terms of the covariance matrix elements iff the matrix itself is expressed in the form of Eq. (10) of Ref. [39]

$$\sigma = \begin{pmatrix} n_1 & 0 & c_1 & 0 \\ 0 & n_2 & 0 & c_2 \\ c_1 & 0 & m_1 & 0 \\ 0 & c_2 & 0 & m_2 \end{pmatrix}, \quad (17)$$

with the matrix elements satisfying the constrains (11a) and (11b) of Ref. [39] that, for the SQL equal to $\frac{1}{2}$, read

$$\begin{aligned} \frac{n_1 - 1/2}{m_1 - 1/2} &= \frac{n_2 - 1/2}{m_2 - 1/2}, \\ |c_1| - |c_2| &= \sqrt{(n_1 - 1/2)(m_1 - 1/2)} - \sqrt{(n_2 - 1/2)(m_2 - 1/2)}. \end{aligned} \quad (18)$$

In this case the EPR operators pair of Eq. (15) are rewritten as

$$\hat{u} = a_0 \hat{x}_1 + \text{sgn}(c_1) \frac{1}{a_0} \hat{x}_2 \text{ and } \hat{v} = a_0 \hat{p}_1 - \text{sgn}(c_2) \frac{1}{a_0} \hat{p}_2,$$

where $a_0 = \sqrt{\frac{m_1 - 1/2}{n_1 - 1/2}} = \sqrt{\frac{m_2 - 1/2}{n_2 - 1/2}}$ with the sufficient and necessary Duan criterion given by

$$a_0^2 (n_1 + n_2 - 1) + \frac{m_1 + m_2 - 1}{a_0^2} - 2(|c_1| - |c_2|) < 0. \quad (19)$$

We note that, as proved in Ref. [39], any Gaussian state can be transformed into the form (17) by local linear unitary Bogoliubov operations, *i.e.* by acting independently on one or both the subsystems by applying local squeezing and/or rotations.

In a more general fashion it is possible to write the sufficient but not necessary condition of Eq. (16) for a **CM** in the standard form of Eq. (2) as

$$(2n - 1) a^2 + \frac{(2m - 1)}{a^2} - 2(c_1 - c_2) < 0,$$

where a can be set to $a^2 = \sqrt{\frac{m - 1/2}{n - 1/2}}$ to minimize the left hand side of the inequality:

$$\sqrt{(2n - 1)(2m - 1)} - (c_1 - c_2) < 0. \quad (20)$$

We note that, while for symmetric states ($m = n$) $|a| = 1$ and the EPR pair consists of two orthogonal field quadratures, this is not true, in general.

The Duan criterion is strictly related to the Heisenberg principle for the single sub-system. If the state is separable the indeterminacy on a single operator is disjoint from the indeterminacy of the twin operator on the second sub-system; so that the total indeterminacy cannot violate the Heisenberg limit. This has nothing to do with conditional measurement and with the possibility of gaining information on one sub-system measuring the other. As we will see this approach leads to a stricter criterion: the so-called EPR "Reid" criterion.

3. The EPR "Reid" criterion

A stronger bound can be found by analysing a bi-partite state under the shadow of conditional measurements. This concept descends directly from the original EPR *gedanken* experiment [2]. For this reason it is usually indicated as the EPR criterion and was firstly introduced by Reid in 1989 [16], in the very early days of quantum information. It describes the ability to deduce the expectation value of an observable on a sub-system by measuring the EPR companion observable on the second sub-system. The EPR "Reid" criterion sets, as the Duan one in its generic form (20), only a sufficient condition for assessing entanglement.

Mathematically this criterion can be deduced by calculating the conditional variance for an observable on sub-system 1 given the result of a measurement on sub-system 2 and comparing it with the standard quantum limit.

For Gaussian states it can be written in terms of **CM** elements:

$$n^2 \left(1 - \frac{c_1^2}{nm}\right) \left(1 - \frac{c_2^2}{nm}\right) < \frac{1}{4}. \quad (21)$$

We note that, being based on conditional variances (and thus on conditional states) this last criterion is not symmetric under the exchange of the two sub-systems. This asymmetry reveals itself in an asymmetric sensitivity to loss [44]. Then, the criterion itself can be recast if sub-system 1 is measured and the conditional variance on 2 is given

$$m^2 \left(1 - \frac{c_1^2}{nm}\right) \left(1 - \frac{c_2^2}{nm}\right) < \frac{1}{4}.$$

The two definitions of the EPR criterion can make it ambiguous if one of the relations are not satisfied. This is not the case of balanced systems ($m = n$). Moreover, it can be proved that no pure state can asymmetrically violate the EPR criterion. At the same time this asymmetry can be useful for revealing eavesdropping in one-sided device-independent QKD schemes [45].

It is easy to see that the above two expressions for the EPR criterion are invariant for symplectic transformations like the PHS one (see Eq. (14)).

The EPR criterion is necessary and sufficient for assessing the "steering" form of nonlocality as recently discussed in Refs. [14, 17]. This concept is very recently gaining much attention as a peculiar consequence of entanglement [46]. It is interesting to note that the concept of conditional variance, used for quantum steering, was used for assessing state preparation ability in quantum demolition experiments [47]. In that case steering happens between the probe and the signal systems.

4. Witnesses

All the above criteria (14), (20), and (21) cannot be used other than as bounds. They are not suitable for measuring entanglement in a quantitative way. Quantifying entanglement for mixed states is a complicated issue still under discussion. There isn't, to date, a single, universal measure that quantifies the entanglement for a mixed state.

In discussing the experimental results in Sect. VI, we will make use of three different witnesses, one each for the above criteria, in order to evaluate their behaviours under lossy transmission:

$$\begin{aligned} w_{PHS} &= 4(nm - c_1^2)(nm - c_2^2) + \frac{1}{4} - (n^2 + m^2) - 2|c_1 c_2|, \\ w_{DUAN} &= 2\sqrt{\left(n - \frac{1}{2}\right)\left(m - \frac{1}{2}\right)} - (c_1 - c_2), \\ w_{EPR} &= n^2 \left(1 - \frac{c_1^2}{nm}\right) \left(1 - \frac{c_2^2}{nm}\right) - \frac{1}{4}. \end{aligned} \quad (22)$$

The three w 's don't satisfy the requirements for being a measure of entanglement. For example they don't verify the basic axiom stating that a good measure should be equal to 0 for any separable state [48].

In summary, for a Gaussian bi-partite state the three criteria (see Eqs. (14), (20), and (21)) reduce to

$$\rho \text{ is entangled } \left\{ \begin{array}{l} \iff w_{PHS} < 0 \\ \iff \left\{ \begin{array}{l} w_{DUAN} < 0 \\ w_{EPR} < 0 \end{array} \right. \end{array} \right. . \quad (23)$$

However, once the state ρ is entangled w_{PHS} , w_{DUAN} and w_{EPR} provide suitable markers for evaluating how far the state is from being separable, somehow measuring the robustness of the entanglement.

Eventually we note that for *diagonal* fully symmetric states ($n = m$ and $c_1 = -c_2 = c$ in Eq. (2)) w_{PHS} , w_{DUAN} and w_{EPR} read

$$\begin{aligned} w_{PHS} &= 4(n^2 - c^2)^2 + \frac{1}{4} - 2n^2 - 2c^2, \\ w_{DUAN} &= \left(n - \frac{1}{2}\right) - c, \\ w_{EPR} &= n^2 \left(1 - \frac{c^2}{n^2}\right)^2 - \frac{1}{4}; \end{aligned}$$

and the two bounds ($c > n - 1/2$) for w_{PHS} and w_{DUAN} coincide while the bound for w_{EPR} is $c > \sqrt{n(n - \frac{1}{2})}$ so that the EPR criterion is stricter than the PHS and Duan ones for any allowed value of n .

B. Quantifying entanglement

The quality of an entangled state can be, indeed, evaluated, operatively, by looking at the effectiveness such a state could, in principle, give in quantum communication protocols. To this end we use \mathcal{F} , the fidelity of CV teleportation of a coherent state, as a benchmark. In fact, \mathcal{F} for a Gaussian resource depends only on the entanglement quality of the resource itself. Using as resource a Gaussian two-mode state described by the **CM** in Eq. (2), \mathcal{F} is given by [49]

$$\mathcal{F} = (1 + m + n - 2c_1)^{-\frac{1}{2}} (1 + m + n + 2c_2)^{-\frac{1}{2}}. \quad (24)$$

It is possible to show that a teleportation protocol of a coherent state, fully based on classical strategies, provides $\mathcal{F} \leq 1/2$. Then, $\mathcal{F} > 1/2$ implies that the resource is entangled. So that, the value of \mathcal{F} becomes an indicator of the quality of the entanglement. We note that for *diagonal* states ($n = m$ and $c_1 = -c_2 = c$) $\mathcal{F} = (1 + 2n - 2c)^{-1} = (2 + w_{DUAN})^{-1}$. In this particular case, perfect fidelity would be obtained for $w_{DUAN} = -2$ that would imply an unphysical **CM** so that Gaussian resources, as the state produced by OPOs, cannot guarantee perfect teleportation [50]. Moreover, $\mathcal{F} > 1/2$ gives $c > n - 1/2$ and coincides with both the Duan and PHS bounds (see the end of the previous subsection) for such *diagonal* states. We note that, similarly to the Duan (Eq. (20)) but contrarily to the PHS and EPR criteria (Eqs. (14) and (21)) \mathcal{F} is not invariant under symplectic transformations.

As already mentioned, only the PHS criterion can be written for a generic **CM** as a sufficient and necessary condition while the Duan and the EPR ones set only sufficient bounds. In order to discuss the relations between the different bounds and the teleportation fidelity, as an entanglement marker, it is possible to draw a region plot, similar to the one drawn in Ref. [51] for a different case. In Fig. 1, we have visualized the different bounds set by the three entanglement witnesses of Eq. (22) and the region for which $\mathcal{F} > 1/2$ (see Eq. (24)). The plot has been computed considering a **CM** in the form of Eq. (2) with $m = n$ (balanced system). The axes report the value of \tilde{c}_1 (below) and \tilde{c}_2 (left), the two correlation terms of the covariance matrix are normalized to $c_{MAX} = \sqrt{n^2 - 1/4}$ so that $\tilde{c}_1 = -\tilde{c}_2 = 1$ represents a pure maximally entangled state (*i.e.* the state showing the maximum quantum correlation for a given total energy of the system). We note that fully symmetric states, that we indicated as *diagonal* states, lay on the plot diagonal (top-left to bottom-right). These states, besides their symmetry, can be obtained at the end of a lossy propagation, described by Eq. (8), of an initially pure state. On the contrary, states outside the diagonal, having $\tilde{c}_1 \neq -\tilde{c}_2$, cannot be obtained by propagating pure states. As a matter of fact, CV entangled states produced by type-II OPO, show, in view of the symmetry in the interaction Hamiltonian, $\tilde{c}_1 = -\tilde{c}_2$. This is not true for CV entangled states obtained by mixing the outputs of two independent type-I OPOs. In such a case the two fields have disjoint Hamiltonians and the symmetry is broken.

The *light gray* (labelled with (VI)) areas indicate un-physical states *i.e.* **CMs** violating inequality (4).

Diagonal states satisfy the conditions (see Eq. (18)) for which the Duan criterion becomes also necessary so that the coincidence between the Duan and the PHS bounds, along the diagonal, is not a surprise. Being both necessary and sufficient they coincide. For these *diagonal* states entanglement (seen as non-separability property) implies $\mathcal{F} > 1/2$. So that entanglement is a pre-requisite for using the state as a resource for the teleportation of a coherent state.

There are two interesting regions in the plot that deserve some comments. The first one, encompassing areas labelled as (III) and (IV) in the plot (*lights green* and *blue*), represents states that violate the PHS bound ($w_{PHS} < 0$) while they do not the Duan one ($w_{DUAN} \geq 0$). This apparent ambiguity can be solved noting that the **CMs** relative to these regions do not respect the condition (18) so that the non-negativity of w_{DUAN} does not imply a separability

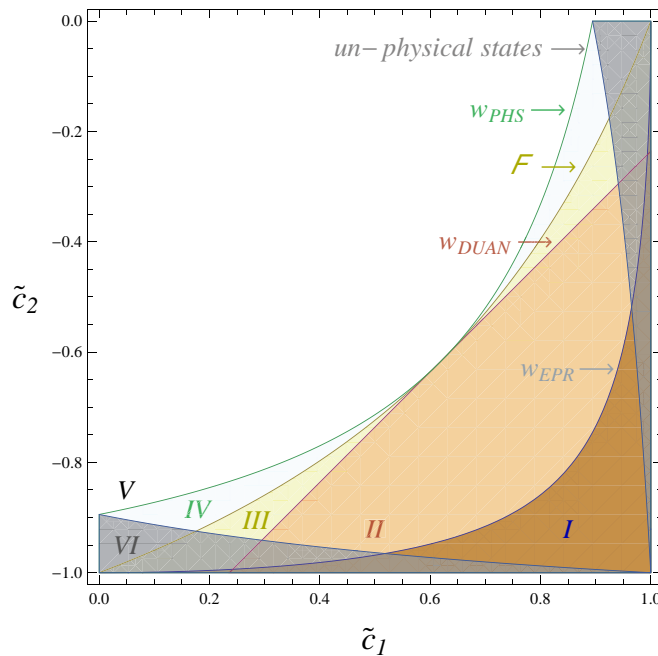


FIG. 1: Region plot (*color online*) of the different entanglement witnesses of Eqs. (22) and teleportation fidelity (Eq. (24)) as an entanglement marker. The *light gray* (labelled with (VI)) areas indicate un-physical **CMs** (*i.e.* violating inequality (4)). The different criteria show different regions of entanglement (see text for details).

of the state. On the other hand for such states $w_{PHS} < 0$ implies that they are effectively entangled and that their density matrix ρ cannot factorize into a convex combination of the tensor product of density operators relative to the two different sub-systems. It is possible to see that if these **CMs** are transformed by local squeezing operations, as outlined in Ref. [39], into a form that fulfills conditions (18), the transformed states show $w_{DUAN} < 0$. We have numerically done a few tests on such *odd* matrices, verifying that once taken into that form, the states violate the Duan bound (19). We note that, being the latter written in a more general form, it is more useful from the practical point of view.

The second interesting region, labelled with (IV) (*light green*) in Fig. 1, represents states that, although entangled, cannot be used for teleporting coherent states. **CMs** lying inside this area will not give $\mathcal{F} > 1/2$. It is interesting to note that such states fall also inside the region for which the Duan criterion (20) is not fulfilled. As above mentioned, once the relative **CMs** are transformed into the form (17) by local squeezing the transformed state will fulfill the Duan criterion in the form (19) so that, in this new scenario, the system will be entangled. At the same time, if this novel state is used as a quantum resource for teleportation of a coherent state it will give $\mathcal{F} > 1/2$ [49] so that local squeezings unveil entanglement. The initial state lying in this area is entangled for PHS, being $w_{PHS} < 0$, but, from the point of view of teleportation, entanglement manifests itself in an useless way. This entanglement can be made useful by locally transforming the two subsystems.

We can see that the EPR criterion (region (I), *light brown*) offers a more restrictive condition with respect to the other two criteria even for diagonal states.

Region (II) (*salmon*) represents the bound fixed by the Duan criterion as a sufficient but not necessary condition. While region (V) (*white*) represent separable states.

1. Mutual information and quantum discord

Recent studies have shown that some particular classes of separable correlated states, traditionally considered classical, show quantum features useful for application in quantum technology [52].

In statistical theory any correlation between two random variables A and B can be measured by their *mutual information* defined by two equivalent expressions:

$$\begin{aligned}
 I(A; B) &\equiv H(A) + H(B) - H(A, B) \\
 &\equiv H(A) - H(A|B) = H(B) - H(B|A)
 \end{aligned}
 \tag{25}$$

where $H(X)$ is the Shannon entropy (the classical analogue of the $S(\rho)$, von Neumann entropy defined in Sect. III 1) associated to the statistical distribution of the variable X ((X, Y) indicating the joint probability distribution and $(X|Y)$ the conditional distribution of Y given the value of X). These two definitions, translated into the quantum language by substituting H with $S(\rho)$, the von Neumann entropy, do not coincide anymore [53]. So, while the translation of the first one into the quantum language is straightforward and univocal, this is not true for the second one.

The first of the two definitions (25), is unambiguously referred to as the quantum mutual information [54] between state 1 and 2 (ρ representing the state of the bi-partite system as a whole)

$$\mathcal{I}(\rho) = S(\rho_1) + S(\rho_2) - S(\rho) . \quad (26)$$

where $\rho_{1(2)} = Tr_{2(1)}[\rho]$ are the partial traces. It relies only on the quantum state of the whole system compared with the single sub-systems' states. In a bi-partite system, described by a density matrix ρ , $\mathcal{I}(\rho)$ quantifies the total correlation between the subsystems ρ_1 and ρ_2 . It is > 0 for entangled states, while it is strictly $= 0$ for separable systems. It can be written in terms of the **CM** invariants (see Sect. II) and symplectic eigenvalues (see Eq. (5))

$$\mathcal{I}(\sigma) = f(n) + f(m) - f(d_+) - f(d_-) , \quad (27)$$

with $f(x)$ given in Eq. (12).

The second definition of Eq. (25), translated into the quantum world, necessarily involves the conditional state of a subsystem after a measurement performed on the other one. So that, the symmetry between the two subsystems is broken. Since the conditional entropy $H(A|B)$ requires to specify the state of B given the state of A , its definition, in quantum theory is ambiguous until the to-be-measured observables on A are selected so that the conditional state of B can be defined.

This discrepancy has led to the concept of quantum discord $\mathcal{D}(\rho)$ [55]. A non zero $\mathcal{D}(\rho)$ signals the presence of quantum features in the correlation between the two sub-systems notwithstanding their separability or entangled nature. So that $\mathcal{D}(\rho)$ is a measure of genuine quantum correlation

$$\mathcal{D}(\rho) = \mathcal{I}(\rho) - \mathcal{C}(\rho) ,$$

where $\mathcal{C}(\rho)$ is the amount of genuinely classical correlation.

For a Gaussian state described by the **CM** (2), \mathcal{D} becomes [53]

$$\mathcal{D}(\sigma) = f(m) - f(d_+) - f(d_-) + f\left(\frac{n + 2nm + 2c_1c_2}{1 + 2m}\right) . \quad (28)$$

We note that, as for the EPR criterion, in quantum discord there is an asymmetry in the exchange of the two sub-systems. Again this is due to the use of the concept of conditional states.

IV. QUANTUM MARKERS EVOLUTION

As shown the **CM** of a bi-partite state undergoing to a lossy transmission evolves as Eq. (9). Consequently the different quantum markers evolve as:

$$\begin{aligned} \mu_T &= \frac{1}{4\sqrt{\det[\sigma_T]}} , \\ \mathcal{F}_T &= \frac{1}{\sqrt{\sqrt{1 + (m_T + n_T)^2 + 2(c_{2,T} - c_{1,T})(1 + m_T + n_T) + 2(m_T + n_T - 2c_{1,T}c_{2,T})}}}} , \\ w_{PHS,T} &= n_T^2 + m_T^2 + 2|c_{1,T}c_{2,T}| - 4(n_T m_T - c_{1,T}^2)(n_T m_T - c_{2,T}^2) , \\ w_{DUAN,T} &= \sqrt{(2n_T - 1)(2m_T - 1)} - (c_{1,T} - c_{2,T}) , \\ w_{EPR,T} &= n_T^2 \left(1 - \frac{c_{1,T}^2}{n_T m_T}\right) \left(1 - \frac{c_{2,T}^2}{n_T m_T}\right) - \frac{1}{4} , \\ \mathcal{I}_T &= f(n_T) + f(m_T) - f(d_{+,T}) - f(d_{-,T}) , \\ \mathcal{D}_T &= f(m_T) - f(d_{+,T}) - f(d_{-,T}) + f\left(\frac{n_T + 2n_T m_T + 2c_1 c_2}{1 + 2m_T}\right) \end{aligned} \quad (29)$$

where the subscript T indicates the quantity undergone to a lossy transmission described by Eq.(9).

We note that the vacuum state obtained for $T = 0$ is a pure one *i.e.* $\mu_0 = 1$. Moreover, in the ideal case (no loss), the OPO would generate a pure state as well. Being $\mu_T < \mu_{0,1}$, for $T \neq 0, 1$, the evolution of μ_T is not monotonic. The purity of the composite system cannot be considered a general entanglement marker [56]. As a matter of fact, any pair of physical systems in a pure state have $\mu = 1$ even if they are disentangled. On the other hand, in our specific case, having a precise hypothesis on the ideal state (a pure twin-beam diagonal state) outing the OPO crystal allows us to consider μ as a measure of the total decoherence that has affected the state.

It is easy to see that \mathcal{F}_T , $w_{PHS,T}$, and $w_{DUAN,T}$ describe properties very robust under decoherence. Once $\mathcal{F} > 1/2$, $w_{PHS} < 0$ and $w_{DUAN} < 0$ for $T = 1$ they will keep breaking the respective bounds for every level of loss. Both mutual information and quantum discord show, with respect to loss, the same feature even if decoherence affects their amount. On the contrary a state that show EPR-like correlation ($w_{EPR} < 0$) for $T = 1$ will not keep this property along the propagation so that some particular protocol based on this property cannot be reproduced. Under a total loss greater than 50% any state loses this correlation property.

V. THE EXPERIMENT

The transmission over a Gaussian channel is described by Eq. (7). As already mentioned this evolution is in all equivalent to a fixed amount of loss introduced by a fictitious beam-splitter. The actual experimental apparatus is made of the CV entangled state source, a variable attenuator (mimicking the BS), and a state characterization stage. A block diagram of the experimental setup is presented in Fig. 2

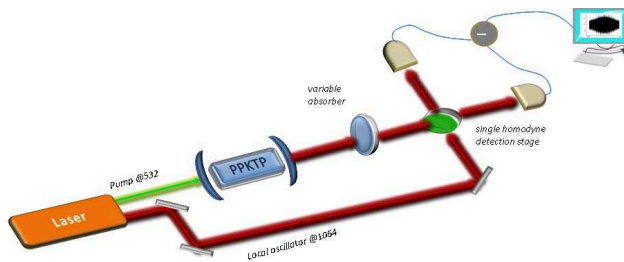


FIG. 2: (*color online*) Block diagram of the experimental setup. The details on the OPO source are given in Ref. [57], while the characterization stage, based on a single homodyne detector, is fully described in Ref. [40].

A. CV entangled state source

The state source relies on a CW internally frequency doubled Nd:YAG laser (Innolight Diabolo) whose outputs @532nm and @1064nm are respectively used as the pump for a non degenerate OPO and the local oscillator (LO) for the homodyne detector. The OPO is set to work below the oscillation threshold and it provides at its output two entangled thermal states (the signal a and the idler b).

The OPO is based on an α -cut periodically poled KTP non linear crystal (PPKTP, *Raicol Crystals Ltd.* on custom design) which allows implementing a type II phase matching with frequency degenerate and cross polarized signal and idler beams, for a crystal temperature of $\approx 53^\circ\text{C}$. The transmissivity of the cavity output mirror, T_{out} , is chosen in order to guarantee, together with crystal losses (κ) and other losses mechanisms (T_{in}), an output coupling parameter $\eta_{out} = T_{out}/(T_{in} + \kappa)$ @1064 nm of ≈ 0.73 , corresponding to an experimental linewidth of 15 MHz @1064 nm. In order to obtain a low oscillation threshold, OPO cavity geometry is set to warrant simultaneous resonance on the pump, the signal and the idler [57]. Measured oscillation threshold is around 50 mW; during measurement runs the system has been operated at $\approx 60\%$ of the threshold power to avoid unwanted non-Gaussian effects [58].

The two beams outing the OPO are transmitted through a filter of variable optical density that mimics the BS. The loss level introduced by the filter is polarization independent and can be tuned from a few percent up to more than 99%.

B. Characterization stage

The signal and idler modes are then sent to the covariance matrix measurement set-up: this consists in a preliminary polarization system, that allows choosing the beam to be detected and a standard homodyne detector. The polarization system is made of an half-wave plate ($\lambda/2$) followed by a polarizing beam splitter (PBS); the different wave-plate orientations allow choosing the beam to be transmitted by the PBS: the signal (a), the idler (b) or their combinations $c = \frac{1}{\sqrt{2}}(a + b)$ or $d = \frac{1}{\sqrt{2}}(a - b)$. Two other combinations, $e = \frac{1}{\sqrt{2}}(ia + b)$ and $f = \frac{1}{\sqrt{2}}(ia - b)$, can be obtained by inserting before the PBS an additional quarter wave plate ($\lambda/4$) [40]. Acquisition times are considerably short thank to pc-driven mechanical actuators that allow setting the $\lambda/2$ and $\lambda/4$ positions in a fast and well calibrated manner.

Once a beam is selected, it goes to an homodyne detector put downstream the PBS. This exploits, as local oscillator, the laser output @1064 nm, previously filtered and adjusted to match the geometrical properties of the OPO output: a typical interferometer visibility is 0.98. The LO phase θ is spanned to obtain a 2π variation in 200 ms. In order to avoid low frequency noise the homodyne current is demodulated at $\Omega=3$ MHz and low-pass filtered ($B=300$ KHz). Then it is sampled by a PCI acquisition board obtaining 10^6 pts/run, with 14-bit resolution. The electronic noise floor is 16 dBm below the shot noise level, corresponding to $\text{SNR} \approx 40$. Data are analysed by a ©Mathematica routine that extract from the six homodyne traces the relevant quadrature variances necessary for reconstructing the whole covariance matrices [40].

VI. EXPERIMENTAL RESULTS

We have performed different sets of measurement under lossy transmission in order to investigate different loss regimes. Each experimental **CM** comes from seven homodyne traces: the shot noise calibration trace, obtained by obscuring the OPO output, six traces each for one of the six modes required for a full state characterization. Contrarily to other previous experiments, where quantum tomographic routine were used in order to retrieve experimental **CMs** [13], we have evaluated **CMs** by a simpler ©Mathematica routine that calculates relevant second order moments of homodyne distributions in a faster way without enhancing the experimental indeterminacy on the **CM** elements. We have tested on a few **CMs** that this procedure gives results in all compatible with quantum tomography. We have also checked, with the standard procedure outlined in [59], that the states under scrutiny were effectively Gaussian.

Once a **CM** is obtained the different entanglement witnesses (w_{PHS} , w_{DUAN} , and w_{EPR} Eqs. (22)), state purity (μ Eq. (11)), teleportation fidelity (\mathcal{F} Eq. (24)), quantum discord (\mathcal{D} Eq. (28)), and mutual information (\mathcal{I} Eq. (26)) are calculated. Then, the overall decoherence, *i.e.* the total level of loss that includes OPO cavity escape efficiency, propagation loss, filter absorption, homodyne efficiency, is assigned as a label to the measurement [22]. This expected level of decoherence is then compared to the theoretical one obtained by inverting Eq. (9) and solving for T under the condition $\det(\sigma_1) = 1/16$; thus requiring that σ_1 represents a pure state (see the discussion at the end of Sect. II). We have verified that, even if experimental **CMs** do not reproduce exactly *diagonal* states, all of them respect the Duan conditions (18) within experimental indeterminacies. So that for the analysed matrices the Duan witness w_{DUAN} represents a sufficient and necessary condition for entanglement.

In all the reported plots we have considered the less decohered datum (obtained for $T = 0.63$) as a reference so that all the reported theoretical curves are obtained imposing that Eqs. (10) and (29) evaluated for $T = 0.63$ give the measured values.

The total losses we have measured span the interval 37–99% ($0.01 \leq T \leq 0.63$). We note that $T = 0.63$, in absence of extra loss and having a cavity escape efficiency of ≈ 0.73 , implies an overall state detection efficiency of ≈ 0.86 in agreement with an homodyne visibility of 0.98 ± 0.01 , a photodiode (nominal) efficiency of 0.90 ± 0.01 and residual transmission loss between the OPO output mirror and the detector surface of 0.01 ± 0.01 .

In Fig. 3 we report the behaviour vs. T of the averaged correlation term ($(|c_{1,T}| + |c_{2,T}|)/2$ see Eq. (10)). As expected the correlation between the two sub-systems degrades linearly with the total loss ($T \rightarrow 0$). The expected behaviour (full *dark orange* line), obtained by considering the less absorbed **CM** ($T = 0.63$) as a reference, follows quite well the reported data. Actually, data refer to acquisition taken on different days so that, the scattering of the point around that line is more due to source long-term dynamics then to actual deviation from the Lindblad model. At the same time the fact that the points are reasonably close to that line proves that the long term stability of the source can be considered quite good.

As already mentioned, w_{PHS} and w_{DUAN} describe a physical property of the state that is strong under decoherence as proved for lower loss (below 90%) in Ref. [22]. They are symptoms of un-separability, in the sense that the system state cannot be described by a density matrix in the form of Eq. (13) [43]. This can be seen in Figs. 4 and 5 where w_{PHS} and w_{DUAN} are plotted vs. T . We have also enlarged, in the insets the region for strong loss ($T < 0.15$) to prove that, even if the analysed state is very close to a two mode vacuum (the total average number of photon $((n + m - 1)/2)$ reduces to 0.02 ± 0.01) it is still experimentally possible to prove that the state is non-separable. It

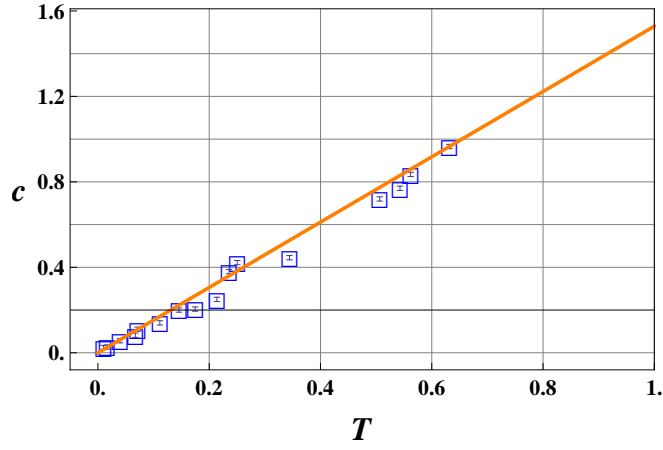


FIG. 3: (*color online*) behaviour of the averaged correlation term $|c_{1,T}| + |c_{2,T}|/2$ in Eq. (9). As expected the correlation reduces linearly with T . The full (*dark orange*) line represents the linear behaviour calculated starting from the first experimental point we have measured ($T = 0.63$). Error bars are smaller than data points and amount to ± 0.01 .

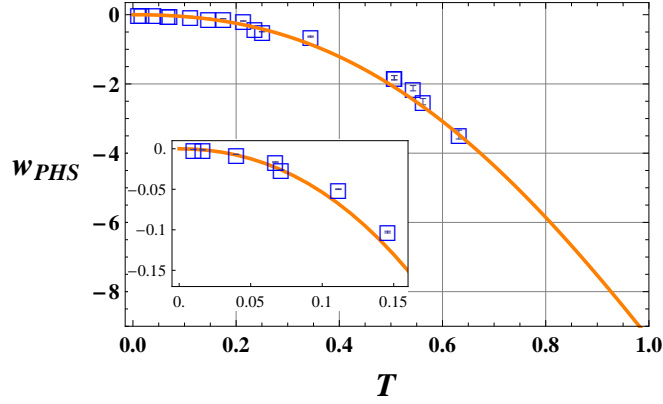


FIG. 4: (*color online*) w_{PHS} vs. T . The full (*dark orange*) line represents the expected behaviour calculated by the third of Eqs. (29) setting the first experimental point at $T = 0.63$ as the initial datum. Error bars, obtained by propagating the experimental indeterminacies in Eq. (22a), range between 10^{-4} and 0.1. In the inset we report the high loss regime ($T < 0.15$) for better enlightning the un-separability, as witnessed by w_{PHS} , even in presence of strong decoherence.

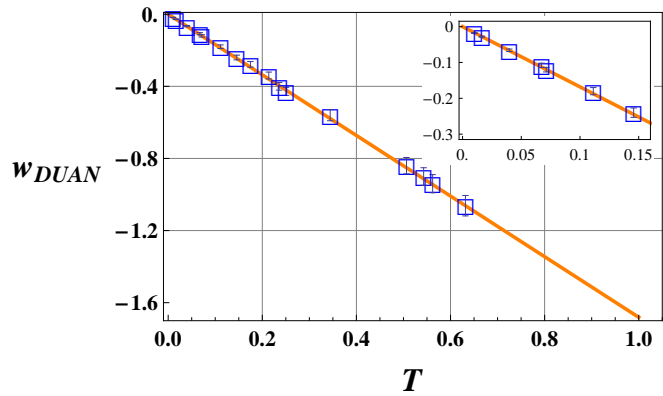


FIG. 5: (*color online*) w_{DUAN} vs. T . The full (*dark orange*) line represents the expected behaviour calculated by the fourth of Eqs. (29) setting the first experimental point at $T = 0.63$ as the initial datum. Error bars, obtained by propagating the experimental indeterminacies in Eq. (22b), range between 0.01 and 0.06. In the inset we report the plot for $T < 0.15$ in order to better visualize the persistence of entanglement, as witnessed by w_{DUAN} , even in presence of strong decoherence.

has to be noted that, while, for $T \rightarrow 0$, w_{PHS} approaches its classical limit non-linearly (see the third of Eqs. (29)), w_{DUAN} (see the fourth of Eqs. (29)) is linear. Thus, in the very high loss regime it becomes more reliable to assess entanglement using the latter than the former.

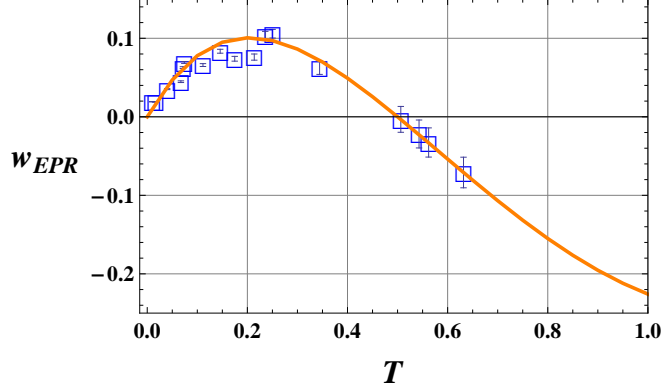


FIG. 6: (*color online*) w_{EPR} vs. T . The full (*dark orange*) line represents the expected behaviour calculated by the fifth of Eqs. (29) setting the first experimental point at $T = 0.63$ as the initial datum. Error bars, obtained by propagating the experimental indeterminacies in Eq. (22c), range between 2×10^{-4} and 0.02. They are considerably larger for point at low losses. As expected for total losses larger than 0.5 $w_{EPR} > 0$ and the state does not show *EPR* correlation.

$w_{EPR} < 0$ indicates that the state exhibits *EPR*-like correlation so that it is possible to gain information on the expectation value of one observable on one sub-system with a precision better than the standard quantum limit once the *EPR* companion is measured on the other sub-system. This feature is by far the most fragile under decoherence: for $T < 0.5$ no state can keep this quantum feature. This can be understood from the fact that loss, a stochastic process, affects directly the degree of correlation between the two sub-systems while the system representation (*i.e.* its un-separability) is only smoothed by this process. It is relevant to note that $T = 0.5$ also corresponds to the minimum state purity μ . So that, losing the *EPR* character coincides with the maximum mixedness for the state during its propagation. In Fig. 6 we report the experimental behaviour found for w_{EPR} for our system. Measured **CM**s for $T < 0.5$ all show $w_{EPR} > 0$. A positive w_{EPR} indicates that, for these states, any attempt to gain information on one sub-system by measuring the other would result less precise than the standard quantum limit.

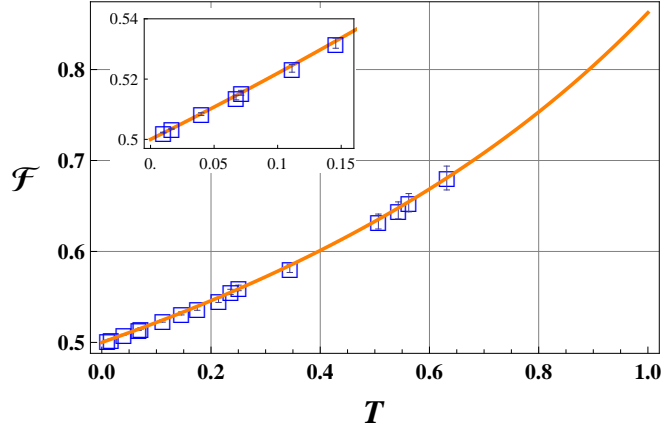


FIG. 7: (*color online*) \mathcal{F} vs. T . The full (*dark orange*) line represents the expected behaviour calculated by the second of Eqs. (29) setting the first experimental point at $T = 0.63$ as the initial datum. Error bars, obtained by propagating the experimental indeterminacies in Eq. (24), range between 10^{-4} and 0.01. In the inset we report the plot for $T < 0.15$ in order to underline the persistence of a quantum teleportation regime even in presence of strong decoherence (high loss) thus proving that even for, in principle, infinite distance this class of states would allow to perform the teleportation of a coherent state with a fidelity above 1/2.

An important signature for an entangled CV state is its ability of acting as a quantum resource in the CV teleportation protocol for coherent state. In Eq. (24) we have expressed the fidelity \mathcal{F} as a function of the **CM** elements. \mathcal{F} , as w_{PHS} and w_{DUAN} , represents a robust signature of quantum properties for the state undergoing to a lossy

transmission. In particular, in Fig. 7, we see that even in the high loss regime, \mathcal{F} remains above the classical limit of 0.5 (see the inset for greater details). Thus proving that CV entangled state, as the one produced by our source, could be used as resource for realising teleportation protocol of coherent state, in principle, at an infinite distance.

Eventually we have retrieved, from our CMs, the value for the quantum mutual information $\mathcal{I}(\sigma)$ (Eq. (27)) and quantum discord $\mathcal{D}(\sigma)$ (Eq. (28)).

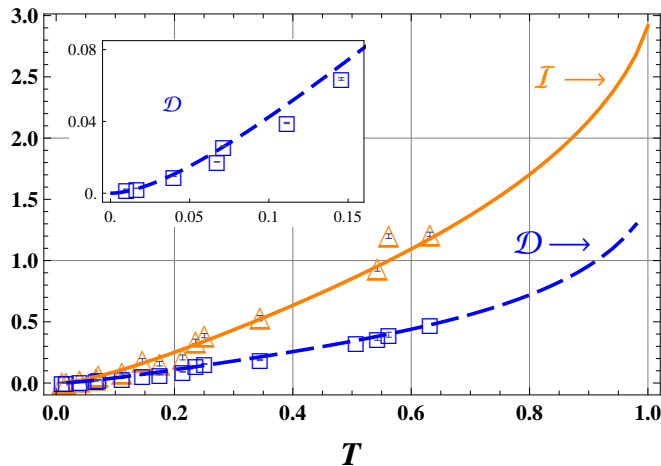


FIG. 8: (*color online*) \mathcal{I} and \mathcal{D} vs. T . The full (*dark orange*) and dashed (*blue*) lines represent the expected behaviours calculated by the sixth and seventh of Eqs. (29) setting the first experimental point at $T = 0.63$ as the initial datum. Error bars, obtained by propagating the experimental indeterminacies in Eqs. (27) and (28), respectively, range between 3×10^{-3} and 0.02 for \mathcal{I} and 10^{-4} and 0.03 for \mathcal{D} . In the inset we report the \mathcal{D} data for $T < 0.15$ in order to underline the persistence of true quantum correlation even in presence of strong decoherence (high loss). Note that the data for \mathcal{I} scatter more from the expected behaviour may be signalling extra classical correlations.

In Fig. 8 we report the experimental data together with the expected behaviours, as usually calculated considering the less decohered matrix as a reference, for \mathcal{I} and \mathcal{D} vs. T . As it can be seen the quantum discord follows very well its *theoretical* line while quantum mutual information is a little more scattered around it. Moreover, our data prove that even in presence of strong decoherence, it is possible to evaluate that \mathcal{D} keeps > 0 , within the experimental indeterminacies, all the way down to an highly absorbed state. We note that Gaussian quantum discord is attracting, very recently, a lot of experimental interest [24, 60, 61]. In particular, in Ref. [24], the authors give an operational significance to quantum discord as the possibility of encoding quantum information in separable states. In Ref. [60] the optimal strategy for evaluating $\mathcal{D}(\sigma)$ in homodyne measurement is presented. It is interesting to compare our experimental plot with the one reported in Ref. [61] where the authors analyse the quantum discord under the lossy transmission of one of the two sub-systems. We note that in their case the scattering of the experimental points around the theoretical curve is almost equivalent for \mathcal{I} and \mathcal{D} while in our case there is a clear difference.

VII. CONCLUSIONS

Gaussian bi-partite states are one of the most renown resources for implementing CV quantum communication protocols such as CV teleportation of coherent states. In this paper we have experimentally analysed how decoherence affects different entanglement criteria and quantum markers for a CV bi-partite state outing a sub-threshold type-II OPO. The decoherence is experimentally introduced by transmitting the quantum state through a variable attenuator. Before illustrating our experimental results we have discussed in details the relationship between the three different entanglement criteria used in the CV framework and linked them to the teleportation fidelity and quantum discord. The latter represent two possible quantum signatures for evaluating the ability of this class of states in quantum communication protocols.

On one hand, our findings prove that the Lindblad approach for describing lossy transmission is valid all the way down to strongly decohered states. On the other hand, with this paper, we prove that the particular class of states we have analysed keeps, within the experimental indeterminacies, its main quantum signatures, *i.e.* the possibility of realizing quantum teleportation of coherent states with a fidelity above 0.5 and a quantum discord above 0 for a total loss of $\approx 99\%$. This proves that the class of CV entangled states, we analysed, would allow, in principle, to realize quantum teleportation over an infinitely long Gaussian channel.

In analysing how quantum discord (see Fig. 8) and quantum mutual information behave under decoherence we interestingly found that the scattering of the points around the theoretical curve is significantly more evident for the quantum mutual information may be signalling that a key role, in our case, is played by unexpected classical correlations. This point will be subject of further theoretical and experimental investigation.

The authors thank S. De Siena and F. Illuminati for useful suggestions and discussions on the theoretical aspects.

-
- [1] E. Schrödinger, Proc. Camb. Philos. Soc. **31**, 555 (1935);
 - [2] A. Einstein, B. Podolsky, and N. Rosen, Phys. Rev. **47**, 777 (1935);
 - [3] Wheeler, J. A., and W. H. Zurek, "Quantum Theory and Measurement", Princeton University Press, Princeton (USA), 1984; A. A. Clerk, M. H. Devoret, S. M. Girvin, Florian Marquardt, and R. J. Schoelkopf, Rev. Mod. Phys. **82**, 1155 (2010);
 - [4] Vittorio Giovannetti, Seth Lloyd, and Lorenzo Maccone, Phys. Rev. Lett. **96**, 010401 (2006); Nat. Photonics, **5**, 222 (2011);
 - [5] Valerio Scarani, Helle Bechmann-Pasquinucci, Nicolas J. Cerf, Miloslav Dušek, Norbert Lütkenhaus, Momtchil Peev, Rev. Mod. Phys. **81**, 1301 (2009);
 - [6] Samuel L. Braunstein and Peter van Loock, Rev. Mod. Phys. **77**, 513 (2005); C. H. Bennet and P. W. Shor, IEEE Trans. of Inf. Theory **44**, 2724 (1998);
 - [7] Timothy C. Ralph and Ping K. Lam, Nat. Photonics **3**, 671–673 (2009);
 - [8] Jeremy L. O'Brien, Akira Furusawa and Jelena Vučković, Nat. Photonics **3**, 687 (2009);
 - [9] A. Serafini, F. Illuminati, M. G. A. Paris and S. De Siena, Phys. Rev. A **69**, 022318 (2004); A Serafini, M.G.A. Paris, F Illuminati and S De Siena, J. Opt. B: Quant. Semiclass. Opt. **7**, R19 (2005);
 - [10] T. Yu, and J.H. Eberly, Science **323**, 598 (2009);
 - [11] P. W. Shor, Phys. Rev. A **52**, 2493, (1995);
 - [12] F. A. S. Barbosa, A. S. Coelho, A. J. de Faria, K. N. Cassemiro, A. S. Villar, P. Nussenzveig, and M. Martinelli, Nat. Photonics **4**, 858 (2010);
 - [13] V. D'Auria, S. Fornaro, A. Porzio, S. Solimeno, S. Olivares, and M.G.A. Paris, Phys. Rev. Lett. **102**, 020502 (2009); D. Buono, G. Nocerino, V. D'Auria, A. Porzio, S. Olivares, and M. G. A. Paris, J. Opt. Soc. Am. B, **27**, A110 (2010);
 - [14] H. M. Wiseman, S. J. Jones, and A. C. Doherty, PRL **98**, 140402 (2007);
 - [15] Alain Aspect, Philippe Grangier, and Gérard Roger, Phys. Rev. Lett. **47**, 460 (1981);
 - [16] M. D. Reid, Phys. Rev. A **40**, 913 (1989);
 - [17] E. G. Cavalcanti, S. J. Jones, H. M. Wiseman, and M. D. Reid, Phys. Rev. A **80**, 032112 (2009);
 - [18] D. Cavalcanti, F. G. S. L. Brandão, and M. O. Terra Cunha, Phys. Rev. A **72**, 040303(R) (2005);
 - [19] H.-P. Breuer, F. Petruccione, "The Theory of open quantum systems", Oxford University Press (2002);
 - [20] R. Simon, E. C. G. Sudarshan, and N. Mukunda, Phys. Rev. A **36**, 3868 (1987); R. Simon, N. Mukunda, and Biswadeb Dutta, Phys. Rev. A **49**, 1567 (1994);
 - [21] L. Vaidman, Phys. Rev. A **49**, 1473 (1994); S. L. Braunstein, H. J. Kimble, Phys. Rev. Lett. **80**, 869 (1998);
 - [22] W. P. Bowen, R. Schnabel, P. K. Lam, and T.C. Ralph, Phys. Rev. Lett. **90**, 043601, (2003); Phys. Rev. A **69**, 012304 (2004);
 - [23] Borivoje Dakić, Yannick Ole Lipp, Xiaosong Ma, Martin Ringbauer, Sebastian Kropatschek, Stefanie Barz, Tomasz Paterek, Vlatko Vedral, Anton Zeilinger, Časlav Brukner, and Philip Walther, Nat. Physics **8**, 666 (2012);
 - [24] Mile Gu, Helen M. Chrzanowski, Syed M. Assad, Thomas Symul, Kavan Modi, Timothy C. Ralph, Vlatko Vedral, and Ping Koy Lam, Nat. Physics **8**, 671 (2012);
 - [25] E. G. Cavalcanti, P. D. Drummond, H. A. Bachor, and M. D. Reid, Opt. Expr. **17**, 18693 (2009);
 - [26] Paul G. Kwiat, Klaus Mattle, Harald Weinfurter, Anton Zeilinger, Alexander V. Sergienko and, Yanhua Shih, Phys. Rev. Lett. **75**, 4337 (1995);
 - [27] Z.Y. Ou, S.F. Pereira, H.J. Kimble, and K.C. Peng, Phys. Rev. Lett. **68**, 3663, (1992);
 - [28] Warwick P. Bowen, Nicolas Treps, Roman Schnabel, and Ping Koy Lam, Phys. Rev. Lett. **89**, 253601 (2002);
 - [29] J. Laurat, G. Keller, J. A. Oliveira-Huguenin, C. Fabre, T. Coudreau, A. Serafini, G. Adesso, and F. Illuminati, J. Opt. B: Quantum Semiclassical Opt. **7**, S577–S587 (2005);
 - [30] A. S. Villar, L. S. Cruz, K. N. Cassemiro, M. Martinelli, and P. Nussenzveig, Phys. Rev. Lett. **95**, 243603 (2005);
 - [31] M.J. Collett and C.W. Gardiner, Phys. Rev. A **30**, 1386 (1984);
 - [32] Ling-An Wu, H. J. Kimble, J. L. Hall, and Huifa Wu, Phys. Rev. Lett. **57**, 2520 (1986);
 - [33] Xiaolong Su, Aihong Tan, Xiaojun Jia, Qing Pan, Changde Xie, and Kunchi Peng, Optics Letters **31**, 1133 (2006);
 - [34] Jietai Jing, Sheng Feng, Russell Bloomer, and Olivier Pfister, Phys. Rev. A **74**, 041804(R) (2006);
 - [35] G. Keller, V. D'Auria, N. Treps, T. Coudreau, J. Laurat, and C. Fabre, Opt. Expr. **16**, 9351, (2008);
 - [36] Christian Weedbrook, Stefano Pirandola, Raúl García-Patrón, Nicolas J. Cerf, Timothy C. Ralph, Jeffrey H. Shapiro, and Seth Lloyd, Rev. Mod. Phys. **84**, 621 (2012);
 - [37] A. Peres, Phys. Rev. Lett. **77**, 1413 (1996); Paweł Horodecki, Physics Letters A **232**, 333 (1997);
 - [38] R. Simon, Phys. Rev. Lett. **84**, 2726 (2000);
 - [39] Lu-Ming Duan, G. Giedke, J. I. Cirac, and P. Zoller, Phys. Rev. Lett. **84**, 2722 (2000);

- [40] Virginia D'Auria, Alberto Porzio, Salvatore Solimeno, Stefano Olivares, and Matteo G A Paris, *J. Opt. B: Quantum Semiclass. Opt.* **7** S750 (2005); Alberto Porzio, Virginia D'Auria, Salvatore Solimeno, Stefano Olivares, and Matteo G.A. Paris, *Int. J. Quantum Information*, **5**, 63 (2007);
- [41] P. D. Drummond and M. D. Reid, *Phys. Rev. A* **41**, 3930 (1990);
- [42] Alessio Serafini, Fabrizio Illuminati, and Silvio De Siena, *J. Phys. B: At. Mol. Opt. Phys.* **37**, L21 (2004);
- [43] Reinhard F. Werner, *Phys. Rev. A* **40**, 4277 (1989);
- [44] M. D. Reid, P. D. Drummond, W. P. Bowen, E. G. Cavalcanti, P. K. Lam, H. A. Bachor, U. L. Andersen, *Rev. Mod. Phys.* **81**, 1727 (2009);
- [45] Cyril Branciard, Eric G. Cavalcanti, Stephen P. Walborn, Valerio Scarani, and Howard M. Wiseman, *Phys. Rev. A* **85**, 010301(R), (2012);
- [46] S. L. W. Midgley, A. J. Ferris, and M. K. Olsen, *Phys. Rev. A* **81**, 022101 (2010); D. J. Saunders, S. J. Jones, H. M. Wiseman, and G. J. Pryde, *Nat. Physics* **6**, 845 (2010); *Corrigendum* in *Nat. Physics* **7**, 918 (2011); Devin H. Smith, Geoff Gillett, Marcelo P. de Almeida, Cyril Branciard, Alessandro Fedrizzi, Till J. Weinhold, Adriana Lita, Brice Calkins, Thomas Gerrits, Howard M. Wiseman, Sae Woo Nam, and Andrew G. White, *Nat. Communications* **3**, 625 (2012); A. J. Bennet, D. A. Evans, D. J. Saunders, C. Branciard, E. G. Cavalcanti, H. M. Wiseman, and G. J. Pryde, *Phys. Rev. X* **2**, 031003 (2012); Vitus Händchen, Tobias Eberle, Sebastian Steinlechner, Aiko Sambrowski, Torsten Franzl, Reinhard F. Werner, and Roman Schnabel, *Nat. Photonics* **6**, 596 (2012);
- [47] M. J. Holland, M. J. Collett, D. F. Walls, and M. D. Levenson, *Phys. Rev. A* **42**, 2995 (1990), J.-Ph. Poizat, J.-F. Roch and P. Grangier, *Ann. Phys. Fr.*, **19**, 265 (1994); F. E. Harrison, D. F. Walls, *Opt. Comm.*, **123**, 331 (1996); Hai Wang, Yun Zhang, Qing Pan, Hong Su, A. Porzio, Changde Xie, and Kunchi Peng, *Phys. Rev. Lett.* **82**, 1414 (1999);
- [48] V. Vedral and M. B. Plenio, *Phys. Rev. A* **57**, 1619 (1998);
- [49] S. Pirandola and S. Mancini, *Laser Physics* **16**, 1418 (2006);
- [50] F. Dell'Anno, S. De Siena, L. Albano, and F. Illuminati, *Phys. Rev. A* **76**, 022301 (2007); F. Dell'Anno, S. De Siena, and F. Illuminati, *Phys. Rev. A* **81**, 012333 (2010);
- [51] F. A. S. Barbosa, A. J. de Faria, A. S. Coelho, K. N. Cassemiro, A. S. Villar, P. Nussenzevig, and M. Martinelli, *Phys. Rev. A* **84**, 052330 (2011);
- [52] Animesh Datta, Anil Shaji, Carlton M. Caves, *Phys. Rev. Lett.* **100**, 050502 (2008); B. P. Lanyon, M. Barbieri, M. P. Almeida, and A. G. White, *Phys. Rev. Lett.* **101**, 200501 (2008)
- [53] Paolo Giorda and Matteo G. A. Paris, *Phys. Rev. Lett.* **105**, 020503 (2010); Gerardo Adesso and Animesh Datta, *Phys. Rev. Lett.* **105**, 030501 (2010);
- [54] S. M. Barnett and S. J. D. Phoenix, *Phys. Rev. A* **40**, 2404 (1989);
- [55] Harold Ollivier and Wojciech H. Zurek, *Phys. Rev. Lett.* **88**, 017901 (2001);
- [56] Gerardo Adesso, Alessio Serafini, and Fabrizio Illuminati, *Phys. Rev. Lett.* **92**, 087901 (2004);
- [57] V. D'auria, S. Fornaro, A. Porzio, E.A. Sete, and S. Solimeno, *Appl. Phys. B* **91**, 309 (2008);
- [58] Virginia D'Auria, Antonino Chiummo, Martina De Laurentis, Alberto Porzio, and Salvatore Solimeno, *Opt. Express* **13**, 948 (2005); V. D'Auria, C. de Lisio, A. Porzio, S. Solimeno, Javid Anwar, and M. G. A. Paris, *Phys. Rev. A* **81**, 033846 (2010);
- [59] J. Řeháček, S. Olivares, D. Mogilevtsev, Z. Hradil, M. G. A. Paris, S. Fornaro, V. D'Auria, A. Porzio, and S. Solimeno, *Phys. Rev. A* **79**, 032111 (2009);
- [60] Rémi Blandino, Marco G. Genoni, Jean Etesse, Marco Barbieri, Matteo G.A. Paris, Philippe Grangier, and Rosa Tualle-Broui, arXiv:1203.1127v3 [quant-ph] 11 Jun 2012;
- [61] Lars S. Madsen, Adriano Berni, Mikael Lassen, and Ulrik L. Andersen, *Phys. Rev. Lett.* **109**, 030402 (2012).